This article is from the
July-August 2009 issue of

CEREAL CHEMISTRY

published by
AACC International, Inc.

For more information on this and other topics
related to cereal science,
we invite you to visit AACC*net* at
www.aaccnet.org

Cross-Sectional Staining and Surface Properties of DDGS Particles and Their Influence on Flowability

Rumela Bhadra,[1] Kurt A. Rosentrater,[2,3] and K. Muthukumarappan[4]

ABSTRACT

Cereal Chem. 86(4):410–420

With the U.S. fuel ethanol industry projected to grow during the next several years, supplies of distillers dried grains with solubles (DDGS) are anticipated to continue to grow as well. DDGS is used primarily as livestock feed. Much of the DDGS must be shipped, often over large distances, outside the Corn Belt (which is where most of the corn-based ethanol plants are currently located). Stickiness and caking among particles is a common issue for DDGS, and it often leads to flowability problems. To address this, the objective of this study was to understand the cross-sectional and surface natures of DDGS particles from five ethanol plants, and how they interact with DDGS properties. This study examined the distribution patterns of chemical components within cross-sections, within section edges (i.e., surface layers), and on surfaces using standard staining techniques; chemical composition was determined using standard protocols; and physical and flowability properties were also determined.

Crude protein in the samples was 28.33–30.65% db, crude fat was 9.40–10.98% db, and neutral detergent fiber (NDF) was 31.84–39.90% db. Moisture contents were 4.61–8.08% db, and geometric mean diameters were 0.37–0.52 mm. Cross-sectional staining showed protein levels of 19.57–40.39%, and carbohydrate levels of 22.17–43.06%, depending on the particle size examined and the production plant from which the DDGS was sampled. Staining of DDGS particles indicated a higher amount of surface layer protein compared with carbohydrate thickness in DDGS particles that had a lower flow function index (which indicated potential flow issues). Additionally, surface fat staining suggested that higher surface fat also occurred in samples with worse flow problems. This study represents another step toward understanding why DDGS particles stick together during storage and transport, and will hopefully help to improve DDGS material handling strategies.

Distillers dried grain with solubles (DDGS) is one of the key coproducts of a typical corn based dry milling bioethanol production plant. It has been estimated that ≈85% of all energy consumed in the United States is from fossil fuel sources (U.S. DOE 2007) and this is expected to rise to meet growing energy demands. Fossil fuel consumption will be dominated by China and India in future years due to exponential growth in population and expanding economies. As fossils-based fuels are nonrenewable, and the supply will eventually diminish, it is very important to find renewable and greener sources of energy. Thus there has been a tremendous potential and need for growth in the bioethanol industry in the past decade, and it is anticipated to increase in future years.

Corn is a predominant cash crop in the Midwest region of the United States, and it is widely used to produce bioethanol for motor fuels. An exponential increase in the corn-based ethanol industry, and thus DDGS, has occurred over the last several years. During fuel ethanol processing, each bushel of corn (≈56 lb) is converted to ≈17 lb of DDGS and 17.6 lb of ethanol, along with a similar quantity of carbon dioxide (Jacques et al 2003). There was nearly 15 million tons of DDGS produced by the end of 2007 in the United States due to the contributions of newly constructed ethanol plants (AAFC 2007). This level is anticipated to be even greater in coming years. To maintain sustainability and viability in the ethanol industry, it is important to augment and increase the use of DDGS in both international and national domains, as only a portion of the DDGS is currently being used in the Midwest,

which is the locus of ethanol manufacturing (NASS 2007). DDGS mainly consists of nonfermented starch and sugars, proteins, fibers, lipids, minerals, water-soluble vitamins, and amino acids. Due to its high energy content, DDGS is used extensively as livestock feed for ruminants and nonruminants. DDGS typically contains ≈86–93% (db) dry matter, 26–34% (db) crude protein, and 3–13% (db) fat (Rosentrater and Muthukumarappan 2006). However, fat percentages are most often in the range of 8–12%.

Because DDGS is often transported in rail cars from the Corn Belt to livestock facilities throughout the nation, as well as international locations, shipping, handling, and storage of DDGS is crucial. During railcar unloading, DDGS flowability is often restricted due to the agglomeration and hardening of DDGS particles. This phenomenon is known as caking and results in bridges among the particles. Often these cakes are broken using a sledge hammer on the outside of the rail car. To limit potential damage to railcars, United States rail carriers have created regulations and restrictions regarding transport of DDGS.

Several factors may influence flowability, such as excessive moisture content, fat levels, temperatures, humidity, or variations in the levels of these factors. Additionally particle size, shape, and nature of surfaces can also affect particle interactions and flow. However, there is not a complete understanding of how an individual factor influences flowability, let alone several factors combined. Additionally, there is some amount of anecdotal knowledge about DDGS flowability from various sources in the industry, but there is a lack of complete understanding (Rosentrater and Giglio 2005; Rosentrater 2006a,b). In terms of scientific studies on DDGS flowability, only a handful of investigations have been published to date. Ganesan et al (2008a) examined the effects of moisture content and soluble level and found that dispersibility, flowability index, and floodability index worsened as moisture and soluble levels increased. Ganesan et al (2008b), again found that increased moisture and soluble levels resulted in decreased flowability, and the addition of a flow agent ($CaCO_3$) (which can also be called an anticaking agent) did not help. In another study, DDGS flowability was modeled using exploratory data analysis techniques to investigate data obtained from experimental measurements and was able to predict a simple model ($R^2 = 0.93$ and SE = 0.12) by combining important flow properties obtained from conventional Carr (1965) and Jenike (1964) tests using response surface modeling and dimensional analysis (Ganesan et al 2007a).

However, that particular study was performed on DDGS samples from a single commercial plant. Samples used in that laboratory-scale study were prepared using mixtures of DDG and CDS (condensed distillers solubles) at various levels. Thus, much more work is needed to completely understand DDGS flowability.

Flowability problems in DDGS may also arise from synergistic effects of environmental factors like humidity and temperature changes), time, compaction, pressure distribution throughout the product mass, chemical components (such as fat and sugar content), and other inherent material properties (particle size, roughness, shape) or variations in the levels of these factors (Craik and Miller 1958; Johanson 1978; Moreya and Peleg 1981; Teunou et al 1999; Fitzpatrick et al 2004a,b). Some of these environmental issues can be remediated with flow conditioning agents, also known as anticaking agents. Even though Ganesan et al (2008b) did not find flow improvement when $CaCO_3$ was added to DDGS, other researchers have successfully worked with other flow agents. For example, the use of calcium stearate and SDS have improved the flow properties in powders such as sucrose, lactose, and modified starch (Chen and Chou 1993; Onwulata et al 1996).

Previous work related to humidity and temperature in terms of DDGS flowability has examined the dynamic water absorption characteristics of DDGS using four soluble levels (10, 15, 20, and 25% db) at four temperatures (10, 20, 30, and 40°C) with four relative humidity levels (60, 70, 80, and 90%) (Ganesan et al 2007c). This study was able to develop a comprehensive adsorption model, the GRM model ($R^2 = 0.94$ and $F = 16503.90$), which was based on soluble levels, relative humidity, and temperature effects, along with time and moisture content. Such a model is beneficial in predicting the dynamic adsorption characteristics of water in to DDGS for different storage conditions. In an another study by the same authors (Ganesan et al 2008c), they were able to predict the sorption isotherm behavior of DDGS, again with varying soluble levels (10, 15, 20, and 25% db) and relative humidity levels (60, 70, 80, and 90%) and they determined the equilibrium moisture content (EMC) for each experimental condition. This study observed that the modified Halsey and modified exponential models performed well for the isotherm data, but an empirical model, the GMR model ($R^2 = 0.94$ and $F = 977.55$) was the best fit for the DDGS under investigation.

Some work has been done on lowering the fat content of DDGS by removing the corn oil, which may improve the marketability of DDGS by increasing the total protein content. Moreover, corn oil from DDGS can be used as a substrate for biodiesel (GS Agrifuels 2006). Use of corn oil for biodiesel production can provide more diversity in the corn processing industry, but on the other hand, removing oil or fat from DDGS will alter the chemical and nutritional properties and may also affect physical and flowability properties as well. Unmodified DDGS and deoiled DDGS samples have been studied for flowability properties using Carr testing and Jenike shear testing (Ganesan et al 2007b). In this work, the reduced fat DDGS did not show significantly fewer flowability problems compared with regular DDGS. However, it should be noted that the reduction of fat in these DDGS samples was done through solvent extraction, and such reduction takes place from within and on the surfaces of particles. Studying the surface fat and other chemical compounds distributions may be an interesting opportunity to examine potential flowability effects.

Beyond moisture content, relative humidity, and moisture sorption patterns, chemical composition can also play a key role in functionality, dispersibility, and flowability of food powders (Pisceky 1997). For example, Perez and Flores (1997) indicated that a high fat content ($\approx 20\%$) in spray-dried soy milk produced worse flow in the resulting milk powder. Additionally, confocal scanning laser microscopy (CLSM) revealed that spray-dried whole milk protein had very little surface fat compared with either a cream powder with high free fat content or a roller-dried milk powder, thereby affecting the flowability (Auty et al 2001).

Microscopic visualization of surface fat globules and coalesced fat has been studied extensively with the help of labeling selective fluorescent probes in milk powders and has greatly improved the understanding of the flowability of such powders (Buma 1968, 1971; McKenna 1997). Studies were also done in milk powders to estimate the effects of surface phospholipids localizations using fluorescently labeled phosphatidylcholine probes with rhodamine filter block at 568 nm (McKenna 1997). These studies revealed the effect of temperature on phospholipids and their effect on flowability. Sensory and instrumental techniques to measure the surface roughness and texture have also been studied, especially for food powders because these properties directly influence consumer preferences. However, these studies can also provide valuable information regarding the surface nature of particles and possible influences on flowability (Chen 2007).

Examination of small particles (such as milk and chocolate powders) requires the use of CLSM, a modern form of light microscopy. Observing small particles with light microscopy will typically produce a blurred image due to a large depth of focus, but this problem can be remediated by the use of confocal laser microscopy (Heertje et al 1987; Brooker 1991, 1995; McKenna 1997). Modern CLSM often contains combined krypton-argon lasers that can produce light at 488, 568, and 614 nm, which allow multiple fluorescent dyes to be excited. Thus, food samples that are dual-labeled for protein and fat can be viewed simultaneously by the use of such laser techniques (Brooker 1995). Commonly used stains are potassium iodide for staining starch (to indicate the amylose chains in blue-black) or amylopectin (red-brown color) (Gaonkar and McPherson 2006). Fats are typically stained slowly with either a Sudan series stain or Nile Red. Standard protocols for fat staining, such as oil red, oil propylene glycol, or osmonium tetraoxide methods for frozen fat sections and phospholipids, are commonly reported in the literature (Landing et al 1952; Pearse 1955; Mallory 1961). The pH of the solution, temperature changes, presence of salts, and concentration of stain molecules are some of the key factors that affect the binding capacity of the stain to food or tissue matrix.

Hematoxylin and eosin stains are frequently used for examining protein tissues. Harris (1900) hematoxylin, Delafield (1885) hematoxylin, Ehrlich (1886) hematoxylin, and Weigert (1904) hematoxylin are common dye solutions (Bancroft and Gamble 2002). Plasma stains like eosin are most frequently anionic (negatively charged) dyes that combine with cationic (positively charged) tissue groups like basic amino acids such as arginine, histidine, and lysine. Eosin typically imparts pink shades to the tissue or cells that contain these amino acids, and thus are used to locate proteins. The counter-stain hematoxylin imparts blue color, indicating the presence of cell nuclei. Periodic Acid Schiff (PAS) staining is often used to stain carbohydrates, especially neutral polysaccharides such as glycogen, starch, cellulose, and chitin; it can also impart a magenta color to glycoproteins and glycolipids (Carson 1926; Stoward 1967).

There is no documented study on the surface composition or characteristics of DDGS particles or their possible relationship to flowability problems. Many investigations have used staining for various food particles but so far none have examined DDGS. Caking (or bridging) phenomena between particles are surface processes and involve physical as well as chemical attributes. Thus the objectives of this study were to evaluate the surface characteristics of DDGS particles in terms of chemical components (i.e., protein and fat) using staining methods and to investigate a possible role in the flowability behavior of the DDGS.

MATERIALS AND METHODS

Sample Collection

Because the nature of the DDGS (physical as well as chemical) will be affected by specific production processes (which may vary

from plant to plant), samples of DDGS (≈20 L) were obtained from five commercial ethanol plants across South Dakota. Samples were collected twice, at different dates. The samples were stored in sealed Ziploc plastic bags under normal, ambient room temperature (≈24 ± 1°C) and humidity conditions throughout the duration of the study. The DDGS samples were then segregated based on particle size using a Rotap sieve analyzer (model RX-29, Mentor, OH) using 8, 12, 16, and 20 U.S. standard sieve sizes (2.38, 1.68, 1.19, and 0.84 mm diameter, respectively). Particles from each sieve were collected and used for both cross-sectional staining of protein and carbohydrate.

Proximate Analysis and Physical Properties

Protein content was determined using AOAC method 990.03 (2003) and fat content was determined using AOAC method 920.39 (2003). Total starch was measured following Xiong et al (1990). Ash content was determined using Approved Method 08-01 (AACC International 2000). Acid detergent fiber (ADF), neutral detergent fiber (NDF), and crude fiber analysis were performed with a fiber analyzer (model 200 ANKOM Technology, Macedon, NY). Two replicates were measured for each property, for each batch, from each plant.

The soluble solids content of the DDGS samples were determined using the technique developed by Ganesan et al (2006). Moisture content of each sample was determined using Approved Method 44-19 (AACC International 2000) using a forced convection laboratory oven (Thelco Precision, Jovan, Wincester, VA). The geometric mean diameter and geometric standard deviation of DDGS particles were calculated using ASAE/ANSI standard S319.3 (2004), and the segregation of the particles was accomplished using a Rotap sieve analyzer (Mentor, OH). Five replicates were measured for each physical property, for each sieve size, for each batch, from each plant.

To increase our understanding about how the chemical constituents relate to physical properties and flowability, we compared our results with our previous work on the same DDGS samples (Bhadra et al 2009). Briefly, angle of repose, Hausner ratio, total flowability index, and total floodability index were determined using Carr index testing (1965) using a PTR powder characteristics tester (Hosokawa Micron Powder Systems, Summit, NJ) as described by ASTM D6393 (1999). Flow function indices were determined as described by ASTM D6128 (2006) using a Jenike shear cell unit (ST-5, Jenike and Johanson, Westford, MA).

Cross-Sectional Staining of DDGS Particles

DDGS particles collected from U.S. sieve no. 8 (2.28 mm diameter), 12 (1.68 mm diameter), 16 (1.19 mm diameter), and 20 (0.84 mm diameter) were packed in a microcassette that was placed in an automatic tissue processing unit (Shandon Excelsior R 13506 Thermoelectron, Pittsburgh, PA). After processing, the DDGS particles were embedded in hot paraffin solution and cooled subsequently to hold the particles and for sectioning in later stages. Fine sections of film ≈5 μm thick were cut using a microtome tissue cutter (Leica RM 2125, North Central Instrument, Plymouth, MN) and then placed on positively charged glass micro slides. It was determined that composition changes in the DDGS particles due to the soaking procedure (i.e., before vs. after) were <0.07%.

After preparing the fine cross-sections of DDGS particles, they were then processed (Shandon Varistain 24-4, Cheshire, UK) for automated H&E staining (protein). The processing procedures were performed at the Histology section of the Veterinary Science Department, Animal Disease Research and Diagnostic Laboratory (ADRL), South Dakota State University.

For PAS staining (carbohydrate), each of the above DDGS particles was deparafinized followed by eight sequential steps: 1) section slides were placed in 1% periodic acid for 10 min; 2) the slides were washed well in running tap water for 10 min; 3)

rinsed well in distilled water; 4) placed in Schiff's reagent for 15 min; 5) placed under running tap water for 10 min; 6) counterstained with light green for 20 sec; 7) dipped in 95% ethyl alcohol for 40 sec and then in formula 83 for another 40 sec; 8) each of the micro slides was dried, and then mounted using Anantech mounting media.

Formula 83, mentioned above, is a specially formulated solution used for PAS staining. PAS staining was performed at the Histology section of Veterinary Science Department, Animal Disease Research and Diagnostic Laboratory (ADRL), South Dakota State University. Each of the stained sections of DDGS from specified sieve sizes were observed under an Olympus SZ 10 stereomicroscope with a DP digital camera at the Genomic Core Facility laboratory of South Dakota State University. Each of the DDGS cross-section images were then analyzed using ImageJ (version 1.38×) software (Rasband 1997-2007). Not only were cross-sections examined, but the images were magnified and the compositions within the particle surface layers were also examined. For carbohydrate and protein staining, we used a full factorial design with three factors (5 plants, 2 batches, and 4 sieve sizes) and each of the samples were replicated three times ($n = 3$) for each sample.

Surface Fat Staining of DDGS Particles

The fat labeling for DDGS particles from U.S. sieve no. 200 (0.074 mm diameter) was performed using a fluorescent probe (Nile Red, Sigma Aldrich, St. Louis, MO) and 1,2 propanediol solvent (Sigma Aldrich) at the concentration of 0.02 g/L as discussed in Auty et al (2001). Nile Red, formally known as Nile Blue A oxazone dye, diffuses readily into the lipid or fat phase and becomes strongly fluorescent when excited in the range of 450–500 nm (McKenna 1997). To reduce nonspecific interaction and trapping of the fluorescent dye in between the DDGS particles, it was washed with 1,2 propanediol solvent (Sigma Aldrich) and centrifuged at 10,000 rpm for 10 min. This procedure was done three times for each sample using a Sorvall Legend RT centrifuge (Thermoelectron, Asheville, NC). This reduced spurious or extra fluorescence from the samples and led to more accurate observations. Each time the supernatants were removed and specifically stained, fine DDGS particles were collected from the residue. The DDGS samples were then excited at a wavelength of 488 nm using a fluorescein isothiocyanate block filter of an Olympus Fluroview FV 300 Laser Scanning Confocal Microscope System interface with an IX 81 microscope (Leeds Precision Instruments, Minneapolis, MN). This procedure was performed at the Genomic Core Facility at South Dakota State University. For fat staining, one replicate was used for each of the two batches from each of the five plants ($n = 2$ for each plant) but only particles collected from sieve size 200 (0.074 mm diameter) were used.

Statistical Analyses

For each property, formal statistical data analyses were conducted using Excel v.2003 (Microsoft, Redmond, WA) and SAS software v.8 (SAS Institute, Cary, NC). A general linear models (GLM) procedure was tested for each property to determine whether significant differences existed using a Type I (α) error rate of 0.05; if so, we then conducted an LSD test using a 95% confidence level to determine where those differences occurred. Additionally, Pearson's linear correlations were examined for all collected data to determine whether potential linear relationships existed between the variables in the study.

RESULTS AND DISCUSSION

Proximate Analysis and Physical Properties

Table I presents the overall proximate analysis of the DDGS samples used in this study.

The crude protein was 28.33–30.65% db, and neutral detergent fiber (NDF) was 31.84–39.90% db. These two chemical constituents were highest in terms of content in the DDGS, followed by acid detergent fiber (ADF), total starch, ash, crude fat, and crude fiber. The compositions of protein and fiber contents determined by proximate analysis and by the cross-sectional staining proce-

TABLE I
Proximate Analysis (% db) of DDGS Samples from Commercial Ethanol Plants Used in This Study[a]

Plant	Batch	Crude Protein	Crude Fat	Crude Fiber	Neutral Detergent Fiber	Acid Detergent Fiber	Total Starch	Ash
1	1	29.45A (0.35)	13.4A (0.64)	9.63A (0.07)	33.74A (1.2)	16.91B (1.16)	9.76A (0.19)	12.54A (1.02)
1	2	29.45A (0.07)	10.4B (0.0)	10.22B (1.46)	29.95B (2.75)	14.08A (3.59)	14.00B (0.35)	14.00A (1.02)
Mean		28.33b (1.25)	10.76a (1.00)	9.93a (1.45)	31.84b (4.02)	15.56a (2.29)	11.82a (1.2)	13.27a (3.10)
2	1	29.85A (0.07)	9.15A (2.47)	9.52A (0.67)	40.02A (3.81)	18.25B (2.29)	10.42B (0.44)	13.41B (1.02)
2	2	31.45B (0.35)	10.45B (0.92)	11.29B (1.26)	39.82A (1.96)	12.18A (1.17)	9.23A (0.05)	11.30A (1.02)
Mean		30.65a (1.20)	9.75a (1.05)	10.30a (1.23)	39.90a (3.95)	15.21a (3.95)	9.81a (1.52)	12.84a (2.56)
3	1	30.4A (0.15)	11.10A (0.29)	10.48A (0.80)	39.85B (2.90)	17.83A (1.11)	12.6B (0.21)	16.59B (1.02)
3	2	29.0A (0.42)	10.9A (0.21)	10.15A (1.06)	37.07A (1.28)	17.95A (2.64)	10.6A (0.39)	9.09A (1.02)
Mean		28.70a (1.32)	10.98a (0.95)	10.32a (1.53)	38.46a (4.01)	17.89a (4.01)	11.59a (1.42)	11.52a (3.05)
4	1	31.7B (0.28)	9.5A (0.14)	7.9A (0.57)	35.8A (0.14)	15.6A (0.49)	9.3B (0.29)	4.15B (0.21)
4	2	29.6A (0.28)	9.3A (0.14)	7.8A (0.57)	37.7A (0.07)	15.0A (0.43)	8.8A (0.00)	4.10A (0.28)
Mean		30.65a (1.23)	9.4b (0.16)	7.85b (0.47)	36.73a (1.07)	15.28a (0.49)	9.05b (0.33)	4.13b (0.21)
5	1	32.3A (0.28)	9.15A (0.07)	8.00A (0.70)	38.4A (0.85)	18.0B (0.64)	10.6B (0.21)	4.55A (0.21)
5	2	31.25A (0.07)	9.85A (0.07)	8.8A (1.84)	39.4B (0.64)	16.5A (1.32)	9.55A (0.21)	4.40A (0.21)
Mean		31.78a (0.63)	9.50b (0.41)	8.40b (1.23)	38.88a (0.86)	17.24a (1.12)	10.05a (0.65)	4.48b (0.22)

[a] Values followed by the same lowercase letters indicate there was no significant difference among the plants for a given dependent variable ($P < 0.05$, LSD). Values followed by the same uppercase letters indicate there was no significant difference between the batches in a particular plant, for a given dependent variable ($P < 0.05$, LSD); n = 2 for each plant and each batch. Values in parentheses are ± 1 standard deviation.

TABLE II
Specific Carbohydrate and Protein Composition Results from Cross-Sectional Imaging of DDGS Particles[a]

Plant	Batch (n = 3)	Mean Particle Size (mm)	Total Area (mm²)[b]	Total Carbohydrate Area (mm²)	Carbohydrate Area (% of cross-section)	Total Protein Area (mm²)	Protein Area (% of cross-section)
1	1	2.38	4.02 (0.06)	2.00 (0.00)	49.75a (0.04)	1.22 (0.00)	30.35a (0.02)
1	1	1.68	2.22 (0.00)	0.89 (1.00)	39.93a (0.00)	0.93 (0.00)	41.76a (0.00)
1	1	1.19	1.01 (0.00)	0.55 (0.00)	53.95a (0.30)	0.35 (0.80)	34.27a (0.00)
1	1	0.84	0.53 (0.00)	0.31 (0.89)	58.96a (0.03)	0.12 (0.72)	22.84a (0.23)
1	2	2.38	5.33 (0.10)	1.94 (0.06)	36.36b (0.00)	1.23 (0.03)	23.15b (0.00)
1	2	1.68	2.38 (0.00)	0.93 (0.13)	39.24a (0.09)	0.93 (0.07)	39.03a (0.00)
1	2	1.19	1.41 (0.00)	0.42 (0.00)	29.95b (0.56)	0.40 (0.00)	27.96b (0.00)
1	2	0.84	0.58 (0.40)	0.14 (0.00)	24.77b (0.00)	0.09 (0.02)	16.31b (0.35)
2	1	2.38	4.45 (1.50)	1.24 (0.00)	27.74a (1.23)	1.27 (0.00)	28.52a (0.00)
2	1	1.68	2.13 (0.00)	0.53 (0.22)	24.60a (0.00)	0.55 (0.00)	25.92b (0.01)
2	1	1.19	1.29 (0.45)	0.36 (0.00)	28.15a (0.33)	0.47 (0.80)	36.38a (0.38)
2	1	0.84	0.57 (0.00)	0.15 (0.56)	26.97a (0.12)	0.21 (0.32)	35.76a (0.70)
2	2	2.38	5.32 (0.80)	1.26 (0.00)	23.62b (0.00)	0.80 (0.03)	15.14b (0.04)
2	2	1.68	2.45 (0.00)	0.73 (0.00)	29.93b (1.23)	0.76 (1.01)	30.77a (0.01)
2	2	1.19	1.36 (2.30)	0.45 (0.00)	33.52a (0.04)	0.36 (0.00)	26.19b (0.06)
2	2	0.84	0.81 (0.00)	0.23 (0.15)	27.68a (0.00)	0.32 (0.20)	39.22a (0.00)
3	1	2.38	5.55 (0.40)	2.27 (0.00)	40.85a (0.00)	1.53 (0.17)	27.51a (0.64)
3	1	1.68	2.14 (0.00)	0.65 (0.00)	30.22a (0.00)	0.54 (0.00)	25.30a (0.01)
3	1	1.19	1.05 (0.67)	0.24 (0.32)	22.64b (0.00)	0.24 (0.42)	23.28b (0.00)
3	1	0.84	0.53 (0.00)	0.15 (0.60)	29.39a (0.01)	0.14 (0.00)	27.11a (0.03)
3	2	2.38	5.09 (0.05)	1.41 (0.00)	27.69b (0.33)	0.84 (0.00)	16.50b (0.00)
3	2	1.68	3.21 (0.00)	0.93 (0.00)	29.09a (0.01)	0.95 (1.00)	29.72a (1.03)
3	2	1.19	1.18 (0.00)	0.36 (0.00)	30.45a (0.02)	0.35 (0.07)	29.71a (0.01)
3	2	0.84	0.46 (0.75)	0.13 (0.03)	28.30a (0.01)	0.12 (0.00)	26.50a (0.01)
4	1	2.38	4.14 (0.54)	0.94 (0.00)	22.84a (0.01)	0.95 (0.00)	22.96a (0.01)
4	1	1.68	2.19 (0.00)	0.64 (0.00)	29.45a (0.05)	0.54 (0.50)	24.68a (0.51)
4	1	1.19	1.85 (0.00)	0.54 (1.00)	29.38a (0.00)	0.56 (0.00)	30.45a (0.40)
4	1	0.84	0.55 (0.70)	0.15 (0.49)	26.35a (1.40)	0.15 (0.00)	27.25b (0.36)
4	2	2.38	4.45 (0.02)	1.10 (0.00)	24.82a (0.05)	0.97 (0.00)	21.80a (1.00)
4	2	1.68	2.04 (0.00)	0.46 (0.51)	22.32b (0.47)	0.54 (0.00)	26.63a (0.00)
4	2	1.19	1.03 (0.30)	0.15 (0.00)	14.97b (0.01)	0.31 (0.39)	30.69a (0.02)
4	2	0.84	0.84 (0.00)	0.27 (0.45)	32.02b (0.01)	0.31 (0.00)	36.74a (0.07)
5	1	2.38	4.33 (0.00)	1.24 (0.00)	28.72a (0.20)	1.25 (0.40)	28.92a (0.00)
5	1	1.68	3.06 (0.15)	0.97 (0.00)	31.65b (0.25)	0.71 (0.71)	23.35b (0.00)
5	1	1.19	1.00 (0.39)	0.35 (0.00)	34.38a (0.30)	0.35 (0.00)	34.59a (0.33)
5	1	0.84	0.67 (0.00)	0.23 (0.41)	34.82b (0.00)	0.16 (0.00)	23.11b (0.00)
5	2	2.38	5.38 (0.02)	1.46 (0.00)	27.23a (0.00)	1.66 (0.89)	30.82a (0.80)
5	2	1.68	3.04 (0.51)	1.20 (0.00)	39.58a (0.06)	1.14 (0.00)	37.58a (0.01)
5	2	1.19	1.00 (0.00)	0.22 (0.00)	21.46b (0.83)	0.33 (0.02)	33.13a (2.30)
5	2	0.84	0.79 (0.00)	0.23 (0.08)	29.73a (0.00)	0.21 (0.00)	27.14a (0.18)

[a] Values followed by the same letter are not significantly different between batches of a particular plant, for a particular particle size ($P < 0.05$, LSD). Values in parentheses are ± 1 standard deviation.
[b] Total area represents cross-sectional area of DDGS particles obtained by imaging.

dure were actually very close. Tables II and III give the protein and carbohydrate compositions determined by microscopy. Table III shows the overall carbohydrate composition was 29.88–31.90% (db) and protein composition was 24.56–30.47% (db). Figure 1 presents examples of typical cross-sectional staining images for carbohydrate and protein content.

Some differences were observed in terms of nutritional content between the two procedures. Cross-sectional staining was done for each of the sieve sizes, and then protein and carbohydrate content were determined using software analysis. Software ImageJ calculated the total cross-sectional area of the particles and the area of protein/carbohydrate distribution. Thus, the percentage of protein/carbohydrate present in the cross-section was determined. On the other hand, for proximate analysis, composition was determined on whole DDGS particles, and no separations of particles were done according to sieve sizes, which might be the reason for the slight differences in the protein and carbohydrate results between the staining and proximate analysis.

Table II gives the results of the composition of carbohydrate and protein content in DDGS particles for their respective screen sizes (diameters). There was no definitive trend in the composition among particle size for a particular sample type. For example, plant 3, batch 2 DDGS particles from sieve no. 20 (0.841 mm diameter) had ≈26.50% of protein, while the same sample showed only 16.50% protein for particles at sieve no. 8 (2.38 mm diameter). However, in plant 4, batch 1 and in plant 2, batch 1 we observed a slight change in carbohydrate percentages among the sieve sizes (22.84–29.45% and 24.60–28.15%). These differences in the nutritional compositions between sieve sizes were similar to results stated by Ileleji et al. (2005) and are reflective of nutrient composition depending, at least to some extent, on the particle size distribution (Liu, 2008). In fact, Wu and Stringfellow (1982; 1986) found that chemical constituents varied according to particle size, and this could be exploited to fractionate DDGS. Additionally, we note that there are no fixed zones where protein and carbohydrates resided separately. Instead, they were dispersed throughout the cross-sections as well as throughout the surface layers. This indicates that, at least for the particles sizes that we examined, the protein and carbohydrates are intimately intermingled in the DDGS particles and cannot be readily separated.

Table III presents the average protein and carbohydrate content determined for each sieve size through cross-section staining of DDGS particles. Plant 1 shows a higher carbohydrate content (39.59–46.96 %) compared with the other plant and plant 5 had higher protein content (25.13–33.86%) compared with the other plants The highest carbohydrate content of 43.06% was found in the sieve size 8 (2.32 mm) (plant 1) and highest protein content (40.39%) was found in sieve size 12 (1.68 mm) (plant 1).

Table IV presents physical and particle properties for the DDGS used in this study. The highest geometric mean diameter was found for plant 3, with a mean value of 1.19 mm. Particle size distribution curves for each of the samples are provided in Fig. 2. As shown, there was some slight variation in particle size distributions among the plants, which is why we selected specific size fractions to analyze.

Also, it should be noted that <1% of each DDGS sample was <0.074 mm, the size used for the surface lipid analysis. Moisture content for all sample types was <9% db and soluble level was 11.26–14.80% db. These values were similar to those of Bhadra et al (2009); however, the moisture contents were lower and more consistent than those found by (Rosentrater 2006c). Perhaps this is indicative of a greater level of quality control during DDGS production at the ethanol plants (Rosentrater 2007, 2008). This is important because, according to Ganesan et al (2008a,b), as moisture content increases, DDGS flowability worsens, across a spectrum of flowability parameters. Moreover, all these parameters are affected by quantity of CDS added to the DWG during the drying process (thus the resulting soluble solid levels), drying conditions (temperatures and times) and also size reduction (hammer milling) of raw corn before fermentation.

TABLE III
Mean Carbohydrate and Protein Composition from Cross Sectional Imaging of DDGS Particles[a,b]

Plant	Mean Particle Size (mm)	Total Area (mm^2)[b]	Total Carbohydrate Area (mm^2)	Carbohydrate Area (% of cross-section)	Total Protein Area (mm^2)	Protein Area (% of cross-section)
1	2.38	4.67 (0.72)	1.97 (0.03)	43.06a (7.33)	1.23 (0.01)	26.75a (3.95)
1	1.68	2.30 (0.08)	0.91 (0.02)	39.59a (0.38)	0.93 (0.00)	40.39a (1.50)
1	1.19	1.21 (0.22)	0.48 (0.07)	41.95a (13.14)	0.37 (0.03)	31.12a (3.45)
1	0.84	0.55 (0.03)	0.23 (0.09)	41.86a (18.72)	0.11 (0.01)	19.57c (3.58)
2	2.38	4.88 (0.47)	1.25 (0.01)	25.68b (2.26)	1.04 (0.25)	21.83a (7.33)
2	1.68	2.29 (0.17)	0.63 (0.11)	27.16b (2.82)	0.66 (0.11)	28.34c (2.65)
2	1.19	1.32 (0.04)	0.41 (0.05)	30.83ab (2.94)	0.41 (0.06)	31.28a (5.58)
2	0.84	0.69 (0.13)	0.19 (0.04)	27.32b (0.39)	0.26 (0.06)	37.49a (1.95)
3	2.38	5.32 (0.25)	1.84 (0.47)	34.27ab (7.21)	1.18 (0.38)	22.00a (6.03)
3	1.68	2.67 (0.59)	0.79 (0.16)	29.66b (0.62)	0.75 (0.23)	27.51c (2.42)
3	1.19	1.11 (0.07)	0.30 (0.07)	26.55b (4.28)	0.30 (0.06)	26.49a (3.52)
3	0.84	0.50 (0.03)	0.14 (0.01)	28.85b (0.60)	0.13 (0.01)	26.80bc (0.34)
4	2.38	4.29 (0.17)	1.02 (0.09)	23.83b (1.08)	2.96 (0.01)	22.38a (0.64)
4	1.68	2.12 (0.08)	0.55 (0.10)	25.88b (3.91)	0.54 (0.00)	25.65c (1.07)
4	1.19	1.44 (0.45)	0.35 (0.21)	22.17b (7.89)	0.44 (0.14)	30.57a (0.13)
4	0.84	0.70 (0.16)	0.21 (0.07)	29.19b (3.11)	0.23 (0.09)	32.00ab (5.19)
5	2.38	4.86 (0.57)	1.35 (0.12)	27.98a (0.82)	1.46 (0.22)	29.87a (1.04)
5	1.68	3.05 (0.01)	1.09 (0.13)	35.62ab (4.35)	0.93 (0.23)	30.47b (7.99)
5	1.19	1.00 (0.00)	0.28 (0.07)	27.92b (7.08)	0.34 (0.02)	33.86a (1.66)
5	0.84	0.73 (0.06)	0.23 (0.00)	32.27b (2.79)	0.18 (0.03)	25.13bc (2.20)
Overall mean for each mean particle size (n = 30 for each sieve pore size)						
	2.38	4.81 (0.56)	1.49 (0.92)	30.96A (8.37)	1.17 (0.27)	24.56A (5.40)
	1.68	2.49 (0.43)	0.79 (0.22)	31.58B (5.96)	0.76 (0.21)	30.47C (6.42)
	1.19	1.22 (0.26)	0.36 (0.13)	29.88C (9.98)	0.37 (0.09)	30.67C (3.98)
	0.84	0.63 (0.13)	0.20 (0.06)	31.90A (9.59)	0.18 (0.08)	28.20B (6.85)

[a] Values followed by the same lowercase letters indicate there was no significant difference among the plants for a particular particle size for that property ($P < 0.05$, LSD). (n = 3 for each sieve size/plant/batch; thus n = 6 for each sieve size/plant.) Values followed by the same uppercase letters indicate there was no significant difference between the particle size for all DDGS samples for that property ($P < 0.05$, LSD) (n = 3 for each sieve size/plant/batch; thus n = 30 for each sieve size/plant.) Values in parentheses are ± 1 standard deviation.
[b] Total area represents cross-sectional area of DDGS particles obtained by imaging.

Table V presents some flowability parameters that were reported in our previous study, in which the same commercial DDGS samples were used (Bhadra et al 2009). For plant 1, batch 1 we observed a higher amount of carbohydrate than protein (Table II), and we can clearly observe a lower angle of repose value (35.95°) and a higher Jenike flow function index (4.56), which indicates relatively good flow. According to the classification of flowability (Carr 1965), with an increase in the angle of repose (typically >45°), the potential for flow problems also increases. Particles with an angle of repose of 36–40° should have fairly good flow. According to standard flow classifications (Jenike 1964), a flow function >4 indicates a reasonably good flow, while a flow function value <4 suggests a cohesive granular solid (i.e., the particles stick together). The flow function index is defined as $F = \sigma_1 / \sigma_c$ where σ_1 is the major consolidation stress and σ_c is the unconfined yield stress (which measures the major compressive strength in the material during flow). Classification of powder flowability, based on the flow function index is given in Table VII. Thus, for plant 1, batch 1, there was fairly good flow behavior (intermittent flow).

Total flowability index for all plants and batches was 79.20–82.40, which according to Carr (1965) classification indicates good flow. But, on the other hand, the floodability index was higher than normal levels, which indicated that there may be potential flushing of the DDGS, that is the particles may tend to flow abruptly and sporadically, which can deteriorate the quality of flow and is not desirable. Becuase the Jenike procedure closely relates to actual industrial situations, however, it may be more logical to relate the results of carbohydrate and protein compositions with the Jenike flow function indices instead.

From Tables II and V, in plant 3, batch 1 we obtained higher percentages of carbohydrates (22.64–40.85%) than protein (23.28–27.51%), and higher values of Jenike flow function index at level 1 consolidation (5.57) and level 2 consolidation (5.69), which indicates good flow for these samples. Plant 5, batch 2 (Tables II and V) had a higher amount of protein (minimum value of 27.14%) compared with carbohydrates (minimum value 21.46%) in the DDGS particles, and they also showed relatively lower values of flow function indices for both consolidation levels (3.07 for level 1 and 1.90 for level 2). This suggests potential flow problems for
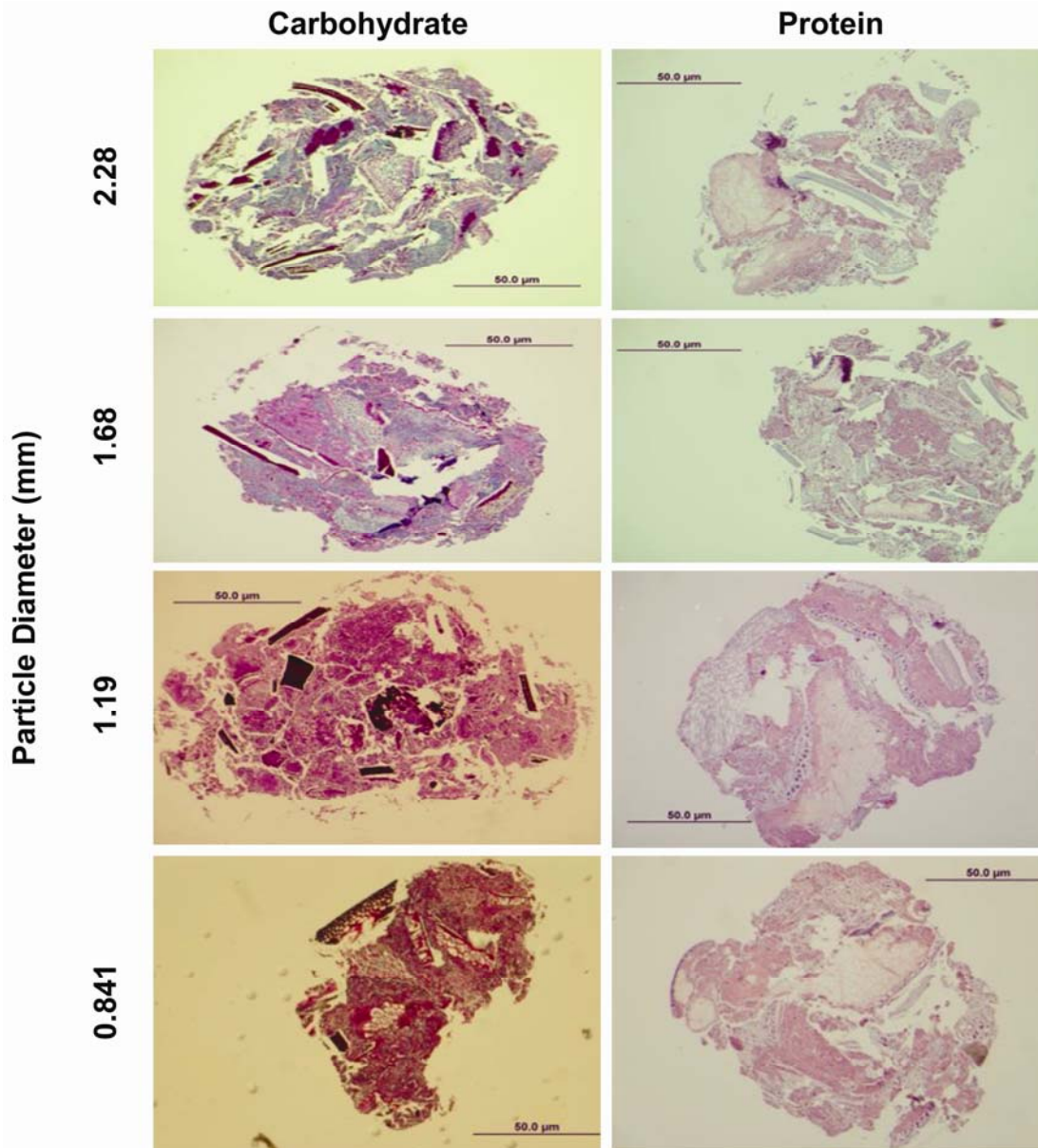

Fig. 1. Representative carbohydrate and protein cross-section images of DDGS particles. Carbohydrate is denoted by dark purple and protein by pink color. (These particles were from Plant 1, Batch 1.) Scale bars are 50 µm in length.

these samples. Again, we observed that for plant 5, batch 1, the protein and carbohydrate composition was very close to the batch 2 levels, and this sample also had low flow functions of 3.28 and 2.18 for level 1 and level 2 consolidation, respectively (Table V). Such low values of flow function indices indicate cohesive flow, according to the Jenike classification.

This indicates that there may be a relationship between the carbohydrate and protein contents in the particles and the resulting flowability in the DDGS.

The authors suggest several possibilities for future work related to flowability and chemical components of DDGS. Proteins could possibly lead to protein-protein or protein-ligand interactions. The physical and flow behavior of DDGS as a function of these types of chemical mechanisms should be investigated. For example,

driving forces involved in intramolecular and intermolecular interactions can be a cause of flow problems in other materials such as whey protein concentrates, milk, and chocolate powders (Gaonkar and McPherson 2006). During changes in environmental conditions like high temperatures, changes in salt concentrations, or concentrations of water molecules, protein can change its conformations and, as a consequence, the reactive amino acids which were previously deep inside the cores of particles may diffuse to the surface to form possible interactions, which may then lead to caking or bridging between reactive particles. Non-polar amino acid residues such as valine, isoleucine, and leucine were previously quantified in DDGS at levels of 1.5, 1.12, and 3.55%, respectively (Spiehs et al 2002). Such nonpolar amino acids are most likely found in the cores of DDGS particles due to hydro-

TABLE IV
Physical Properties of the DDGS Samples from Commercial Ethanol Plants Used in this Study[a]

Plant	Batch ($n = 5$)	Geometric Mean Diameter (d_{gw}, mm)	Geometric Standard Deviation (S_{log}, mm)	Moisture Content (%, db)	Soluble Level (%, db)
1	1	0.83A	0.48A	4.32A (0.65)	12.56A (3.06)
1	2	0.87A	0.55A	4.92A (1.03)	12.77A (2.12)
Mean		0.80ab (0.03)	0.52a (0.05)	4.61b (0.87)	12.56ab (3.06)
2	1	0.79A	0.45A	4.60A (0.88)	11.03A (1.82)
2	2	0.21B	0.30A	5.36A (1.25)	13.73A (2.59)
Mean		0.50b (0.41)	0.38a (0.12)	4.98a (1.10)	12.34b (2.55)
3	1	1.00A	0.45A	5.84A (1.32)	10.58A (1.29)
3	2	1.38B	0.49A	5.38B (1.66)	13.38A (1.16)
Mean		1.19a (0.27)	0.47a (0.03)	5.61b (1.44)	11.98b (1.88)
4	1	0.80A	0.20A	6.42A (0.35)	14.80A (2.82)
4	2	0.81A	0.53A	8.83A (2.54)	14.32A (2.55)
Mean		0.81ab (0.01)	0.37a (0.23)	7.63a (2.13)	14.59a (2.55)
5	1	0.68A	0.47A	7.26A (0.43)	12.26A (1.82)
5	2	0.97B	0.54A	8.89A (3.18)	11.26A (1.40)
Mean		0.83ab (0.21)	0.51a (0.05)	8.08a (2.31)	11.41b (1.54)

[a] Values followed by the same lowercase letters indicate there was no significant difference among the plants for a given dependent variable ($P < 0.05$, LSD). Values followed by the same uppercase letters indicate there was no significant difference between the batches in a particular plant for a given dependent variable ($P < 0.05$, LSD) ($n = 5$ for each plant/batch). Values in parentheses are ± 1 standard deviation.

TABLE V
Some Key Flowability Parameters for DDGS Samples in This Study[a,b]

Sample	Angle of Repose (°)	Hausner Ratio[c] (-)	Total Flowability Index (-)	Total Floodability Index (-)	Flow Function Index[d] (-) Level 1[e]	Flow Function Index[d] (-) Level 2[f]
Plant 1						
Batch 1	35.94B (1.37)	1.09A (0.03)	81.40A (0.89)	63.60A (3.78)	4.56B (2.12)	2.25B (1.39)
Batch 2	40.62A (0.34)	1.08A (0.00)	81.00A (0.00)	63.41A (3.13)	5.35A (0.23)	2.47A (0.56)
Batch mean	38.28b (2.64)	1.08b (0.02)	81.20a (0.63)	63.50a (3.27)	4.96b (0.56)	2.36c (0.16)
Plant 2						
Batch 1	37.76B (0.74)	1.04A (0.04)	82.40A (0.96)	53.52B (0.64)	1.43B (0.25)	1.45A (0.69)
Batch 2	41.60A (1.41)	1.03A (0.01)	80.80B (0.84)	57.47A (1.84)	1.79A (1.10)	1.59A (1.17)
Batch mean	39.68a (2.22)	1.04a (0.02)	81.60a (1.20)	55.35b (2.57)	1.61e (0.25)	1.52e (0.10)
Plant 3						
Batch 1	39.48B (0.64)	1.04A (0.01)	80.80B (0.84)	70.20A (0.45)	5.57A (0.25)	5.69A (0.38)
Batch 2	40.76A (0.85)	1.04A (0.02)	82.10A (1.14)	60.70A (2.41)	4.55B (1.01)	4.83B (1.30)
Batch mean	40.12a (0.98)	1.04a (0.01)	81.45a (1.17)	65.27a (5.27)	5.06a (0.72)	5.26a (0.61)
Plant 4						
Batch 1	37.26A (1.04)	1.03A (0.01)	82.00A (0.71)	70.20A (1.15)	3.47A (0.01)	2.53B (0.70)
Batch 2	38.98A (1.28)	1.08B (0.01)	79.40B (1.29)	62.10A (0.65)	3.27A (2.14)	4.37A (1.70)
Batch mean	38.12b (1.43)	1.06a (0.03)	80.70ab (1.69)	66.15a (4.36)	3.37cd (0.14)	3.45b (1.30)
Plant 5						
Batch 1	39.82A (1.41)	1.05A (0.01)	79.20A (0.76)	48.60B (1.52)	3.28A (0.17)	2.18A (0.10)
Batch 2	38.722 (1.04)	1.06A (0.01)	79.30A (0.45)	64.60A (1.52)	3.07B (0.14)	1.90B (0.25)
Batch mean	39.27ab (1.31)	1.05a (0.01)	79.55b (0.64)	56.85b (8.55)	3.18d (0.15)	2.04d (0.20)

[a] Determined by Bhadra et al (2009).

[b] Values followed by same uppercase letters indicate no significant difference among batches for a particular plant's property ($P < 0.05$, LSD). Values followed by same lowercase letters indicate no significant difference among plants for that property ($P < 0.05$, LSD); $n = 5$ for each plant/batch unless noted otherwise. Values in parentheses are ± 1 standard deviation.

[c] Hausner ratio is defined as the ratio of packed bulk density to aerated bulk density.

[d] $n = 3$ for each plant/batch for this property.

[e] Level 1: 14.5 kg consolidation weight for shear testing procedure (Jenike 1964; Bhadra et al 2009).

[f] Level 2: 3 kg consolidation weight for shear testing procedure (Jenike 1964; Bhadra et al 2009).

phobicity. But the particles can also change surface hydrophobicity due to environmental conditions like heat (Nakai 1983), to which the particles will be exposed during drying. And at very short distances, van der Waals forces can drive proteins to interact. Furthermore, the presence of charged polar amino acids may result in Ca^{2+} bridging, commonly known as salt bridges in proteins. For example, in whey protein powder, there was stability of α-lactalbumin protein when there was an increase in Ca^{2+} (Boye et al 1997). Charged amino acids residues such as histidine, lysine, threonine, and arginine have been quantified in DDGS as well (Spiehs et al 2002). In their study, DDGS from Minnesota and South Dakota were lower in Ca^{+2} content but higher in phosphorous levels. Additionally, these DDGS samples had higher amounts of threonine (1.13%) and arginine (1.2%). Thus, formation of salt bridges with phosphorous or other salts may be possible for the amino acid residues in DDGS and may lead to worse flow problems. The potential for these mechanisms to occur should be investigated.

Along similar lines, aggregation in protein molecules can cause hardening in gels (Mulvihill et al 1988). Hydrophobic interactions and electrostatic charge interactions during protein-protein or protein-ligand interactions plays a fundamental role in attraction of particles (Gaonkar and McPherson 2006). On such an event, two particles with a sufficient moisture film may interact with one another to remove the water molecules (hydrophobic effect) on their surface; thus in this process they can form an aggregate particle, which can lead to flow restrictions on a larger scale. This type of mechanism should also be investigated for DDGS particles.
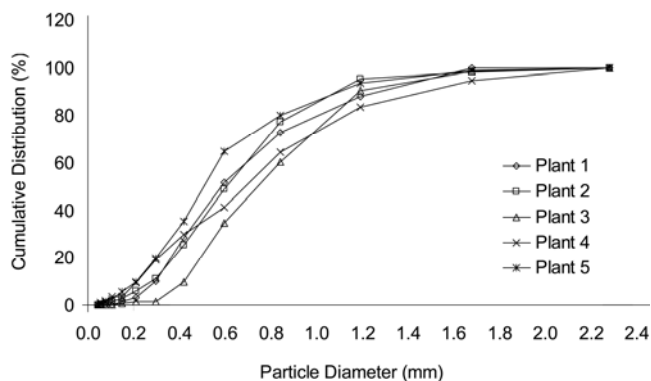

Fig. 2. Particle size distributions of DDGS samples used in the study.

Surface Thickness of Carbohydrate and Protein by Cross-Sectional Staining

Table VI indicates the surface thickness of carbohydrate and protein layers for DDGS particles, but only from sieve no. 8 (2.28 mm diameter). We observed that plant 3, batch 1 had the highest carbohydrate surface thickness (4.80 μm), and it also had the highest Jenike flow function (Table V). Likewise for plant 4, batch 1, we obtained a higher thickness for surface protein (3.21 μm) compared with carbohydrates, and this sample also had a lower flow function index (which indicated more cohesiveness in the DDGS). Higher flow function index (>4) typically indicates good flow in solid materials (Jenike 1964). The presence of higher amounts of protein on the surface compared with carbohydrates appeared to be related to lower flow function index and may be explained due to protein-protein interactions as discussed above. Of course, more investigation is necessary to confirm this possibility.

It should also be noted that there was the presence of blue color counterstain in the H&E stained particles, which indicates the possible presence of nucleic acids. Becuase DDGS is formed as the coproduct of industrial fermentation using yeast, it is probable that yeast proteins, as well as nucleic acid materials from yeast cells, impart blue color due to staining. Negative charges on DNA and nucleic acids from damaged corn and yeast cells can also facilitate electrostatic attraction between DDGS particles, which may lead to aggregation of DDGS particles and potential flow problems.

Ideally DDGS should have low residual starch. During fermentation to ethanol glucose, maltose, and fructose should be fermented to alcohol by the yeast. However, from the samples examined during this study, we have found ≈10% starch content (9.81–11.82%), which indicates some inefficiencies in the manufacturing processes used at the facilities where our samples were collected. It should be noted that the starch analysis method does count all the enzyme hydrolyzable carbohydrates (from triose to starch). The presence of starch molecules in DDGS was also depicted in the PAS staining of polysaccharides in this study. Residual starch can be another reason for particle stickiness and thus flow problems (i.e., starch gelatinization at higher temperatures) during processing and storage, and logically should be the basis for a thorough follow-up investigation.

Surface Fat Through CLSM

Figure 3 shows the presence of fat globules on the surfaces of DDGS particles. Each image was taken at 10× using confocal laser microscopy with a 1/5.6 sec exposure time. For plant 2

TABLE VI
Surface Thickness (μm) of Carbohydrate and Protein Components for 2.28 mm Diameter DDGS Particles[a,b]

Plant	Batch (n= 1)	Diameter (mm)	Carbohydrate		Protein	
			Maximum Thickness	Minimum Thickness	Maximum Thickness	Minimum Thickness
1	1	2.28	3.00	0.25	3.21	1.92
1	2		2.56	0.70	2.57	0.53
Mean			2.78a (0.31)	0.48b (0.32)	2.56b (0.86)	1.23b (0.98)
2	1	2.28	0.65	0.12	0.11	0.00
2	2		0.59	0.20	0.75	0.23
Mean			0.62e (0.04)	0.16e (0.06)	0.75d (2.56)	0.12c (0.16)
3	1	2.28	4.80	2.00	0.57	0.11
3	2		0.40	0.20	1.27	0.23
Mean			2.60bc (3.11)	1.09d (1.28)	1.27c (2.56)	0.23d (0.17)
4	1	2.28	2.50	0.35	3.79	2.53
4	2		0.75	0.21	2.57	0.52
Mean			2.63bc (2.65)	0.28c (0.10)	2.57ab (2.56)	1.53a (1.42)
5	1	2.28	1.25	0.45	0.80	0.35
5	2		1.70	0.75	1.21	0.45
Mean			1.48d (0.32)	0.60a (0.21)	2.56b (0.29)	0.40c (0.07)

[a] Values in parenthesis are ±1 standard deviation.
[b] Mean values followed by the same letter are not significantly different among the plants for that property ($P < 0.05$, LSD).

(batch 1), plant 1 (batch 2), plant 4 (batch 2), and plant 5 (batch 2) we observe fat globules of >10 μm and with a greater concentration of fluorescence. This indicates a higher amount of surface fat on those particles. Surfaces could be clearly observed and the lipids appear to be agglomerated. For plant 2 (batch 1), plant 4 (batch 2), and plant 5 (batch 2), surface fat globules were also observed >10 μm in size, mostly 20–40 μm. We also observe higher concentrations of fat globules in these. Such observations in food powders were related to flow problems (Buma 1968, 1971). From Table V, we clearly see that these DDGS samples had Jenike flow function indices of 1.43, 3.27, and 3.07, respectively. These ranges of flow function index indicate cohesive flow in the DDGS, according to Jenike classification, which is shown in Table VII. Moreover, the fat globules in plant 1 (batch1) were of less concentration and this sample had a Jenike flow function

index of 4.56, which indicates good flow. We observed that plant 1 (batch 2) had relatively large surface fat globules but showed a high Jenike flow function index, which means it had good flow characteristics. Thus, these observations appear to indicate that surface fat could be a possible reason for flow problems in DDGS (or at least it may be related).

The relationship between a higher amount of surface fat and poor flow is logical, as fat molecules on particle surfaces play an important role in flowability for other granular materials. Additionally, fat molecules at high temperatures may liquefy and act as glue between particles, thus leading to stickiness and caking. For example, fat produced worse flow problems in soy milk powders (Perez and Flores 1997). However, plant 1 (batch 2) had the highest amount of fat droplets but a Jenike flow function index of 5.35, which indicates good flow. These kinds of results reveal that
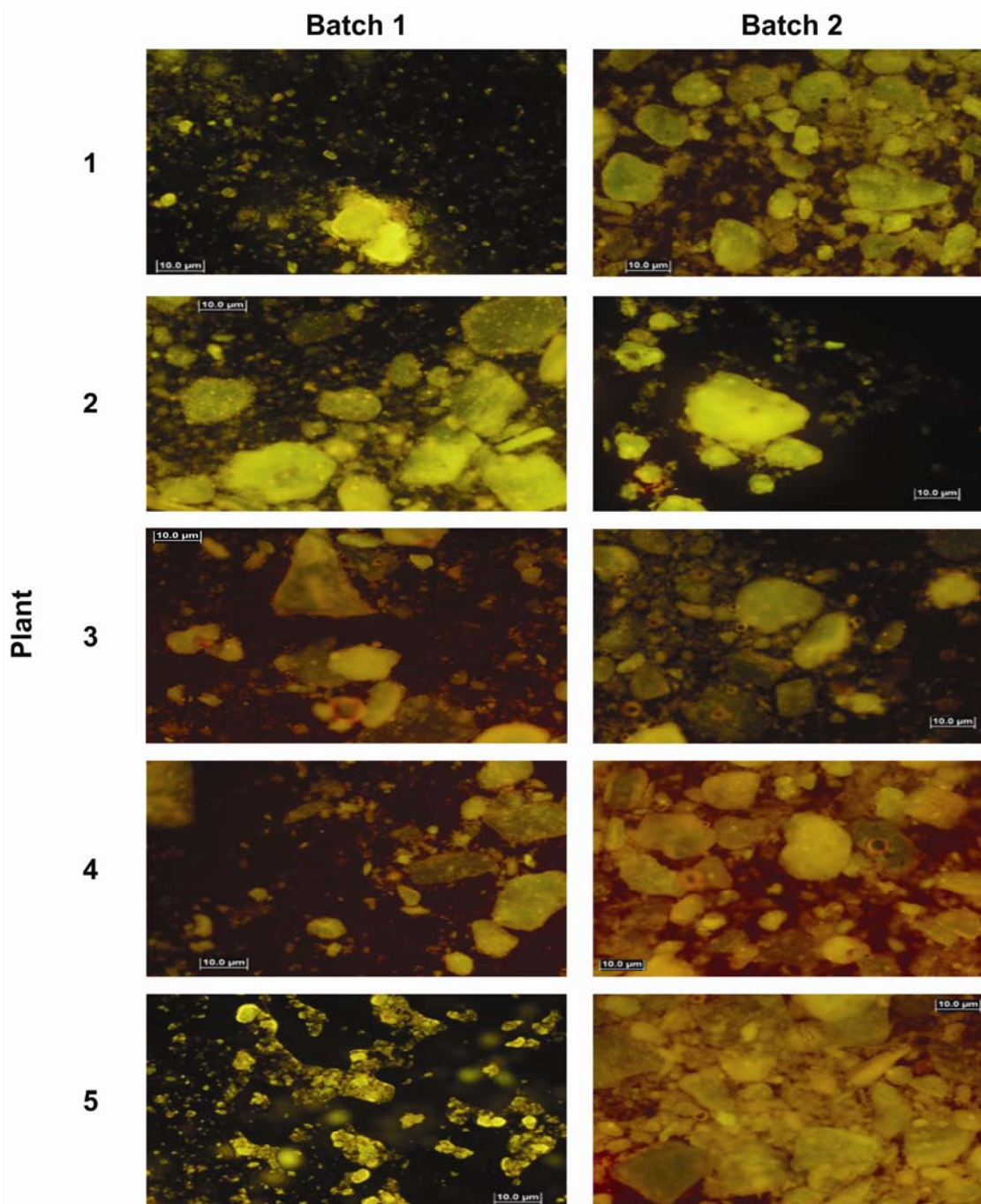

Fig. 3. Representative surface fat images of DDGS particles at 10× magnification. Scale bars = 10 μm. (Particles from a sieve diameter of 0.074 mm.)

flowability is not only dependent on surface fat composition but also on other chemical, physical, and environmental factors.

Surface phospholipid quantification, using specific fluorescent probes, could also estimate their role in agglomeration of DDGS particles. Because DDGS is a biological particle, it is natural that there would be some autofluorescence from the particle itself, even without specific fluorescent probes, when excited with laser. But this kind of microscopic staining research with DDGS particles has not been done yet.

Additional Considerations

It is important to consider whether small particles can be used to describe the behavior of the larger particles in the DDGS, especially in terms of chemical properties. To investigate this question, we conducted a means separation test on all of the chemical constituent data using SAS (LSD at 95% significance level) to determine whether significant differences occurred across all of the sieve sizes (Table VIII). Very few differences due to particle size (little constituent fractionation or concentration) were observed. Thus, it appears that all of the particle sizes used in the study provided an adequate representation of the overall DDGS.

To address the question regarding whether chemical composition (overall, cross-sectional, or surface) is related to the flowability of the DDGS particles, a Pearson's linear correlation analysis (using SAS) was performed on all collected data. Unfortunately, no significant correlations existed between any of the constituents and either physical properties or flowability properties of the DDGS. However, a few other interesting correlations were found. For example, the geometric standard deviation and aerated bulk density had a relatively high linear correlation ($r = -0.7088$), which indicates that the aerated bulk density decreased as the variability in particle size increased. Additionally, dispersibility was inversely related to both the Jenike level 1 flow function index ($r = -0.6847$) as well as the Jenike level 2 flow function index ($r = -0.6607$). This essentially means that as the variability in particle size increased, the flowability of the DDGS decreased. Moreover, the angle of spatula was linearly correlated with the Jenike level 1 flow function index ($r = 0.6781$). This should occur because the angle of spatula should be related to the internal friction between particles. Thus, it appears that, at least for a few properties, Carr testing may be a suitable surrogate for Jenike testing, which could save time and potentially provide a simpler means to determine flowability. This would be an appropriate follow-up investigation, however.

CONCLUSIONS

From this study, it has become evident that higher surface protein and fat levels in DDGS were related to poor flow properties. DDGS flowability appears to be related not only to surface fat and protein, but also to distributions throughout the particle cross-sections, as well as the interactions between these constituents. Microscopic staining techniques combined with image analysis were able to provide quantitative results that can help us better understand the nature of DDGS particles and the causes of flowability problems in DDGS. Greater surface proteins with carbohydrates and greater surface fat appeared to correspond to worse flowability. Additionally, the role of residual starch should be investigated. Because flowability is a multivariate problem, it is important to continue to focus on various aspects of DDGS particles, especially the nature of the surfaces, to determine why they stick together during storage and transportation, and to help guide remediation strategies that ultimately will help to improve DDGS material handling behavior.

LITERATURE CITED

AACC International. 2000. Approved Methods of the American Association of Cereal Chemists, 10th Ed. The Association: St. Paul, MN.

AAFC. 2007. Protein meal: Situation and outlook. Agriculture and Agri-Food Canada Bi-weekly Bulletin 19(3):1-4.

AOAC International. 2003. Official Methods of Analysis of the Association of Analytical Chemists, 17th Ed. Gaithersburg, MD.

ASAE. 2004. S19.3 Method of determining and expressing fineness of feed materials by sieving. ASAE Standards. St Joseph, MI.

ASTM. 1999. D6393. Standard test method for bulk solids characterization by Carr indices. ASTM Standards: W. Conshohocken, PA.

ASTM. 2006. D6128. Standard test method for shear testing of bulk solids using Jenike shear cell. ASTM Standards: W. Conshohocken, PA.

Auty, M. A. E., Twomey, M., Guinee, T. P., and Mulvihill, D. M. 2001. Development and application of confocal scanning laser microscopy methods for studying the distribution of fat and protein in selected dairy products. J. Dairy Res. 68:417-427.

Bancroft, J. D., and Gamble, M. 2002. Theory and Practice of Histological Techniques, 5th Ed. Harcourt: London.

Bhadra, R., Muthukumarappan, K., and Rosentrater, K. A. 2009. Flowability properties of commercial distillers dried grains with solubles (DDGS). Cereal Chem. 86:170-180.

Boye, I., Alli, I., and Ismail, A. A. 1997. Use of differential scanning calorimetry and infrared spectroscopy on the study of thermal and structural stability of α lactalbumin. J. Agric. Food Chem. 45:1116-1125.

TABLE VII
Flow Function Classification According to Jenike (1964)
Shear Testing Methodology

Flow Functions	Classification of Flow
F < 1	No flow
1 < F < 2	Highly cohesive
2 < F < 4	Cohesive
4 < F < 10	Intermittent flow
10 < F	Free flow

TABLE VIII
Mean Composition (% db) According to Particle Size (Pooled Across all Plants)[a]

Particle Size (mm)	0.84	1.19	1.68	2.38
Crude protein	30.11a	29.62b	29.88b	30.99a
Stain-protein	28.20a	30.67a	30.47a	24.57b
Crude fat	9.94a	10.57b	10.52b	11.07b
Stain-carbohydrate	31.90a	29.89a	31.58a	30.92a
NDF	35.46a	33.23b	33.76ab	30.73c
ADF	14.84ab	15.97a	14.98ab	14.01b
Starch	9.71a	10.54ab	11.03bc	11.61c
Ash	4.38a	4.31a	4.48ab	4.63b

[a] Values within a row followed by the same letter are not significantly different among the particle sizes for that property ($P < 0.05$, LSD).

Brooker, B. E. 1991. The study of food systems using confocal laser scanning microscopy. Microscopy Anal. 26:13-15.

Brooker, B. E. 1995. Imaging food systems by confocal laser scanning microscopy. Pages 533-568 in: New Physico-Chemical Techniques for the Characterization of Complex Food Systems. E. Dickenson, ed. Blackie Academic and Professional Publishers: London.

Buma, T. J. 1968. A correlation of free fat content and moisture content of whole milk spray powders. Netherlands Milk Dairy J. 22:22-28.

Buma, T. J. 1971. Free fat in spray-dried whole milk. PhD dissertation. Agricultural University: Wageningen, Netherlands.

Carr, Jr., R. L. 1965. Evaluating flow properties of solids. Chem. Eng. 72:163-168.

Carson, F. L. 1926. Histotechnology–A Self Instruction Text, 2nd Ed. Chapters 6 and 7. Amer. Soc. Clinical Pathologist Press: Chicago, IL.

Chen J. 2007. Surface texture of foods: Perception and characterization. Crit. Rev. Food Sci Nutr. 47:583-598.

Chen, Y. L., and Chou, J. Y. 1993. Selection of anti-caking agents through crystallization. Powd. Technol. 77:1-6.

Craig, D. J., and Miller, B. F. 1958. The flow properties of powders under humid conditions. J. Pharm. Pharmacol. 10:136-144.

Delafield, J. 1885. Zeitschrift für wissenschaftliche Mikrosckopie und für mikroskopishe technik. 2:228.

Ehrlich, P. 1886. Fragekasten. Zeitschrift für wissenschaftliche Mikroskopie und für mikroskopiche Technik. 3:150.

Fitzpatrick, J. J., Barringer, S. A., and Iqbal, T. 2004a. Flow property measurement of food powders and sensitivity of Jenike's hopper design methodology to measured values. J. Food Eng. 61:399-405.

Fitzpatrick, J. J., Iqbal, T., Delaney, C., Twomey, T., and Keogh, M. K. 2004b. Effect of powder properties and storage conditions on the flowability of milk powders with different fat contents. J. Food Eng. 64:435-444.

Ganesan, V., Rosentrater, K. A., and Muthukumarappan, K. 2006. Methodology to determine soluble content in dry grind ethanol coproduct streams. Appl. Eng. Agric. 22:899-903.

Ganesan, V., Rosentrater, K. A., and Muthukumarappan, K. 2007a. Modeling the flow properties of distillers dried grains with solubles (DDGS). Cereal Chem. 84:556-562.

Ganesan, V., Rosentrater, K. A., and Muthukumarappan, K. 2007b. Physical and flow properties of regular and reduced fat distillers dried grains with solubles (DDGS). Food. Bioprocess Technol. 2:156-166.

Ganesan V., Rosentrater, K. A., and Muthukumarappan, K. 2007c. Dynamic water adsorption characteristics of distillers dried grains with solubles. Cereal Chem. 84:555-584.

Ganesan V., Muthukumarappan, K., and Rosentrater, K. A. 2008a. Effect of moisture content and soluble level on the physical, chemical, and flow properties of distillers dried grains with solubles. Cereal Chem. 85:464-470.

Ganesan, V., Muthukumarappan, K., and Rosentrater, K. A. 2008b. Effect of flow agent addition on the physical properties of DDGS with varying moisture content and soluble levels. Trans. ASABE 51:591-601.

Ganesan, V., Muthukumarappan, K., and Rosentrater, K. A. 2008c. Sorption isotherm characteristics of distillers dried grains with solubles (DDGS). Trans. ASABE 51:169-176.

Gaonkar, A. K., and A. McPherson, eds. 2006. Microscopy a tool to study ingredient interactions in food. Chapter 2 in: Ingredient Interactions Effect on Food Quality, 2nd Ed. CRC: Boca Raton, FL.

GS Agrifuels. 2006. GS Agrifuels to convert corn oil into biodiesel to ethanol facilities. Available online: http://www.tmcnet.com/enews/e-newsletters/alternative-power/20061108/u2064140-gs-agrifuels-convert-corn-oil-into-biodiesel-ethanol.htm.

Harris, H. F. 1900. On the rapid conversion of hematoxylin into hematein in staining reactions. J. Appl. Microscopic Lab. Methods 3:777-780.

Heertje, I., Van der Vlist, P., Blonk, J. C. G., Hendricks, H. A. C. M., and Brackenhof, G. J. 1987. Confocal scanning laser microscopy in food research: Some observations. Food Microstructure 6:115-120.

Ileleji, K. E., Stroshine, R. L., and Prakash, K. S. 2005. Segregation during gravity driven discharge of distiller's grain with solubles. ASABE Annual Meeting Paper No: 066115. American Society of Agricultural and Biological Engineers: St. Joseph, MI.

Jaques, K. A., Lyons, T. P., and Kelsall, D. R. 2003. The Alcohol Textbook. University Press: Nottingham, UK:

Jenike, A. W. 1964. Storage and Flow of Solids. Bull. No. 123. Utah Engineering Station, University of Utah: Salt Lake City.

Johanson, J. R. 1978. Know your material—How to predict and use the properties of bulk solids. Chem. Eng./Date Book October 30:9-17.

Landing, B. H., Uzman, L. L., and Whipple, A. 1952. Lab Investigations 1:456-462.

Liu, K. 2008. Particle size distribution of distillers dried grains with solubles (DDGS) and relationships to compositional and color properties. Bioresource Technol. 99:8421-8428.

Mallory, F. B. 1961. Pathological Technique. Hafner: New York.

McKenna, B. A. 1997. Examination of whole milk powder by confocal laser scanning microscopy. J. Dairy Res. 64:423-432.

Moreyra, R., and Peleg, M. 1981. Effect of equilibrium water activity on the bulk properties of selected food powders. J. Food Sci. 46:1918-1922.

Mulvihill, D. M., and Kinsella, J. E. 1988. Gelation of β lactalbumin: Effects of sodium chloride and calcium chloride on the rheological and structural properties of gels. J. Food Sci. 53:231-236.

Nakai, S. 1983. Structure function relationship of food protein with an emphasis on the importance of protein hydrophobicity. J. Agric. Food Chem. 31:676-683.

NASS. 2007. Ethanol coproducts used for livestock feed. Available online www.nass.usda.gov/Statistics_by_State/Iowa/Publications/Annual_Statistical_Bulletin/2007/07_111.pdf. USDA National Statistics Service: Washington, DC.

Onwulata, C. I., Konstance, R. P., and Holsinger, V. H. 1996. Flow properties of encapsulated milk fat powders as affected by flow agent. J. Food Sci. 61:1211-1215.

Pearse, A. G. E. 1955. J. Pathological Bacteria 70:554-557.

Perez, M. F., and Flores, R. A. 1997. Particle size of spray dried soymilk. Appl. Eng. Agric. 13:647-652.

Pisecky, J. 1997. Achieving product properties. Pages149-191 in: Handbook of Milk Powder Manufacture. Niro A/S: Copenhagen.

Rasband, W. S. 2007. ImageJ Bethesda, Maryland. U.S. National Institute of Health. Available online: http://rsb.info.nih.gov/ij/.

Rosentrater, K. A. 2006a. Understanding distillers grain storage, handling and flowability challenges. Distill. Grains Q. 1:18-21.

Rosentrater, K. A. 2006b. Understanding flowability, 2: Some key parameters. Distill. Grains Q. 1:20-23.

Rosentrater, K. A. 2006c. Some physical properties of distillers dried grains with solubles (DDGS). Appl. Eng. Agric. 22:589-595.

Rosentrater, K. A. 2007. DDGS quality: A key to overcoming utilization barriers and misconceptions. Distill. Grains Q. 2:17-19.

Rosentrater, K. A. 2008. DDGS quality, 2: Are you in control? How to quantify your process with control charts. Distill. Grains Q. 3:24-29.

Rosentrater, K. A., and Giglio, M. 2005. What are the challenges and opportunities for utilizing distillers grains? Distill. Grains Q. 1:15-17.

Rosentrater, K. A., and Muthukumarappan, K. 2006. Corn ethanol coproducts: Generation, properties, and future prospects. Int. Sugar J. 108:648-657.

Spiehs, M. J., Whitney, M. H., and Shurson, G. C. 2002. Nutrient database for distiller's dried grain with solubles produced from new ethanol plants in Minnesota and South Dakota. J. Anim. Sci. 80:2639-2645.

Stoward, P. J. 1967. The histochemical properties of some periodate-reactive mucosubstances of a pregnant Syrian hamster before and after methylation with methalonic thionyl chloride. J. R. Microscop. Soc. 87:77.

Subramaniam, P. J., Burke, O. C., Kristott, J. U., Groves, K. H. M., and Jones, S. A. 1994. Heat resistant chocolate. Res. Report No. 710. Leatherhead Food Int.: Surrey, UK.

Teunou, E., Fitzpatrick, J. J., and Synnott, E. C. 1999. Characterization of food powders flowability. J. Food Eng. 39:31-37.

Weigert, K. 1904. Eine Kliene Verbesserung der Hamatoxylin van-Gieson-methode. Zeitschrift für wissenschaftliche Mikroskopie und für mikroskopische.

Wu, Y. V., and Stringfellow, A. C. 1982. Corn distillers' dried grains with solubles and corn distillers' dried grains: Dry fractionation and composition. J. Food Sci. 47:1155-1157, 1180.

Wu, Y. V., and Stringfellow, A. C. 1986. Simple dry fractionation of corn distillers' dried grains and corn distillers' dried grains with solubles. Cereal Chem. 63:60-61.

U.S. DOE (United States Department of Energy). 2007. Available online: http://www.energy.gov/energysources/fossilfuels.htm.

Xiong, Y., Bartle, S. J., and Preston, R. L. 1990. Improved enzymatic method to measure processing effects and starch availability in sorghum grain. J. Anim. Sci. 68:3861-3870.